Self-similar space-time evolution of an initial density discontinuity

V. L. Rekaa, H. L. Pécseli, and J. K. Trulsen

Citation: Physics of Plasmas **20**, 072117 (2013); doi: 10.1063/1.4816953
View online: http://dx.doi.org/10.1063/1.4816953
View Table of Contents: http://aip.scitation.org/toc/php/20/7
Published by the American Institute of Physics

Self-similar space-time evolution of an initial density discontinuity

V. L. Rekaa,[1,a)] H. L. Pécseli,[1,b)] and J. K. Trulsen[2,c)]
[1]*Department of Physics, University of Oslo, Box 1048 Blindern, N-0316 Oslo, Norway*
[2]*Institute of Theoretical Astrophysics, University of Oslo, Box 1029 Blindern, N-0315 Oslo, Norway*

(Received 16 April 2013; accepted 3 July 2013; published online 31 July 2013)

The space-time evolution of an initial step-like plasma density variation is studied. We give particular attention to formulate the problem in a way that opens for the possibility of realizing the conditions experimentally. After a short transient time interval of the order of the electron plasma period, the solution is self-similar as illustrated by a video where the space-time evolution is reduced to be a function of the ratio x/t. Solutions of this form are usually found for problems without characteristic length and time scales, in our case the quasi-neutral limit. By introducing ion collisions with neutrals into the numerical analysis, we introduce a length scale, the collisional mean free path. We study the breakdown of the self-similarity of the solution as the mean free path is made shorter than the system length. Analytical results are presented for charge exchange collisions, demonstrating a short time collisionless evolution with an ensuing long time diffusive relaxation of the initial perturbation. For large times, we find a diffusion equation as the limiting analytical form for a charge-exchange collisional plasma, with a diffusion coefficient defined as the square of the ion sound speed divided by the (constant) ion collision frequency. The ion-neutral collision frequency acts as a parameter that allows a collisionless result to be obtained in one limit, while the solution of a diffusion equation is recovered in the opposite limit of large collision frequencies. © *2013 AIP Publishing LLC*. [http://dx.doi.org/10.1063/1.4816953]

I. INTRODUCTION

A classic dynamic problem in studies of plasma phenomena concerns the space-time evolution of an initial step-like discontinuity of the plasma density. A special limiting case is where plasma expands into vacuum.[1–3] The problem is interesting also for practical reasons: analytical and numerical studies often assume an initial condition to be given, while many laboratory experimental conditions assume some given boundary conditions. A comparison between analytical and experimental results is not always simple in such cases.[4] The step-like initial condition is one that can be realized by an absorbing grid in a streaming plasma, as found in, for instance, a single ended Q-machine.[5–7] Two time scales can be distinguished: first, an initial expansion of the electron component, where the electric field develops due to the charge imbalance caused by the electron pressure. Inertia makes the ion motion negligible on this time scale. Later, we find a slow expansion of the entire bulk plasma density, where also the ions are set into motion by the collective electric fields. The basic elements of the problem can be understood even in a spatially one dimensional analysis, and only this case will be considered here: physically it corresponds to the low frequency dynamics in a strongly magnetized Q-machine plasma, for instance.

A complete understanding of the ion dynamics requires information of the velocity distribution $f(x,u,t)$ for ions with velocities u, at positions x at times t, as described by the ion Vlasov equation for ions with mass M and charge e

$$\frac{\partial}{\partial t}f + u\frac{\partial}{\partial x}f - \frac{e}{M}\frac{\partial\phi}{\partial x}\frac{\partial}{\partial u}f = 0, \tag{1}$$

where $E \equiv -\partial\phi/\partial x$ is the electric field and ϕ is the electrostatic potential. The ion density is $n_i = \int_{-\infty}^{\infty} f\,du$. For the relevant low-frequency dynamics, we can safely assume the electrons to be Boltzmann distributes at all times, so that the electron dynamics are accounted for by the relation $n_e = n_0\exp(e\phi/T_e)$, where T_e is the electron temperature.

For times exceeding the ion plasma period, $t \gg 2\pi/\omega_{pi}$, with ω_{pi} being the ion plasma frequency, and at large scale lengths, we can assume that the plasma dynamics are quasi-neutral, $n_e \approx n_i \equiv n$. In this limit, the Debye length no longer enters the problem, and we have neither constant characteristic length nor time scales in the dynamic equations. (All we have is a velocity, the ion sound speed $C_s = \sqrt{T_e/M}$ derived from the electron temperature.) For such cases, the characteristic scales are determined solely by initial or boundary conditions. Under these conditions, we can expect the plasma dynamics to evolve self-similarly, in depending functionally on the ratio $\zeta \equiv x/t$ rather than on x and t independently,[8–12] giving $\partial/\partial t \to -t^{-2}x\partial/\partial\zeta = -t^{-1}\zeta\partial/\partial\zeta$ and $\partial/\partial x \to t^{-1}\partial/\partial\zeta$. Heaviside's step function or the δ-function are examples of functions without length scales. We thus assume an initial step-like density perturbation. By introducing the variable $\zeta \equiv x/t$, we can then reduce Eq. (1) to

$$(u-\zeta)\frac{\partial}{\partial\zeta}f - \frac{T_e}{M}\frac{1}{n}\frac{\partial n}{\partial\zeta}\frac{\partial}{\partial u}f = 0, \tag{2}$$

[a)]Electronic mail: v.l.rekaa@fys.uio.no
[b)]Electronic mail: hans.pecseli@fys.uio.no
[c)]Electronic mail: j.k.trulsen@astro.uio.no

after a little algebra, where we now have $f=f(\zeta,u)$ and $n=n(\zeta)\equiv\int_{-\infty}^{\infty}f(\zeta,u)du$. The collective electric field was determined by the assumption of Boltzmann distributed electrons, giving $n=n_0\exp(e\phi/T_e)$. From Eq. (2), we have the relation

$$f(u,x,t)=\begin{cases} G_-(u)+C_s^2\int_{-\infty}^{x/t}\frac{1}{n}\frac{\partial n}{\partial\zeta}\frac{\partial f/\partial u}{u-\zeta}d\zeta & \text{for } x/t<u\,,\\ G_+(u)-C_s^2\int_{x/t}^{\infty}\frac{1}{n}\frac{\partial n}{\partial\zeta}\frac{\partial f/\partial u}{u-\zeta}d\zeta & \text{for } x/t>u\,,\end{cases} \tag{3}$$

where $G_-(u)\equiv f(x\to-\infty,u)$, $G_+(u)\equiv f(x\to+\infty,u)$. With the present assumptions, we have $G_-(u)=(n_0+\Delta n)f_0(u)$ and $G_+(u)=n_0f_0(u)$, where we for simplicity introduced the unperturbed velocity distribution in the form $n_0f_0(u)$ with the normalization $\int_{-\infty}^{\infty}f_0(u)du=1$. This form turns out to be convenient when we linearize the equations. The self-similarity of the solutions can also be understood by identifying a dynamic length-scale $\ell\equiv C_st$. The self-similar variable is then recovered by the normalized length $x/\ell\sim x/t$.

The assumption of Boltzmann distributed isothermal electrons is standard for low frequency, long wave-length perturbations and is obtained analytically by ignoring the electron inertia. In this limit, the electron thermal conductivity in effect becomes infinite, and a constant T_e can be argued by a constant electron temperature reservoir present at $|x|\to\infty$ In the model assumed here, the energy for accelerating the ions originates from the ambipolar electric field build-up by the electron pressure. The constant electron temperature reservoir thus serves as a constant energy source. The argument assumes implicitly that no local potential maxima develops, where electrons can be trapped[13] with a velocity distribution deviating from the assumed Maxwellian. We find that for our problem the ion Landau damping is smoothing out small scale potential variations (the "Airy function ripples") so we have a monotonically varying plasma density as long as $T_e/T_i\le 5$, and with this temperature restriction, the analysis is self-consistent.

In the present paper, we study the space-time evolution of a step-like initial condition for the plasma density, with particular attention to the self-similarity of the evolution. We study (both analytically and numerically) the problem under conditions that can be realized in a laboratory experiment, such as a single ended Q-machine.[14] The electron temperature is here determined by the hot end-plate of the device.

.The first part of the analysis considers collisionless plasmas. If a neutral gas is introduced, we will have ion-neutral and electron-neutral collisions modifying the dynamics. Since the basic analysis assumes the electrons to be isothermally Boltzmann distributed at all times, we do not expect electron collisions to give significant modifications of the results. Inclusion of ion-neutral collisions on the other hand introduces a new length scale, the mean free collision length, ℓ_c, and we want to analyze how this new feature modifies the self-similar evolution.

If we take the temperature of the neutral gas at rest to be very low, we find that the ion component can develop two distinct populations:[15] one being the part of the ions accelerated through the potential drop at the boundary and having not yet collided, and a part formed by the charge exchange collisions and appearing as a cold component with no drift velocity. In this case, we can have an ion velocity distribution developing that is unstable to kinetic ion-ion instabilities.[16] This result has interest only for very low neutral temperatures and is not elaborated further here.

The paper is organized as follows: in Sec. II, we present results from an exact solution of the linearized version of Eq. (3) and compare it with numerical results in Sec. III. In Sec. IV, we extend the analysis to include collisions, using a model best suited for charge exchange collisions although we use a constant collision frequency, independent of velocity, to simplify the analysis. Corresponding numerical results are shown in Sec. V. Sections III and V present results from numerical Particle in Cell (PIC) simulations of the problem. The theoretical analysis uses a Maxwellian velocity distribution as a reference since many integrals can be expressed by the plasma dispersion function. The numerical simulations address a physically realizable situation where the velocity distribution evolves by a simulated plasma production at the boundary. Section VI contains our discussions and conclusions.

II. LINEARIZED MODEL

In many cases, an initial value problem can be formulated only in a formal way; it is rather difficult to imagine how to set up an initially prescribed density variation over all space. There are of course several realizable and nontrivial examples, which are interesting for experimental tests of the results. Here, we consider the one dimensional case, where the initial perturbation consists of a step in the ion velocity distribution at $t=0$ giving $(n_0f_0(u)+\Delta ng(u))$ for $x<0$ and $n_0f_0(u)$ for $x>0$, with $\Delta n\ll n_0$ and $\int_{-\infty}^{\infty}f_0(u)du=1$. The analysis allows in principle for having a perturbation of the ion velocity distribution function $\Delta n\,g(u)\neq\Delta nf_0(u)$, but we do not make use of this additional freedom of choice here.[5,17]

The space-time variation of the perturbation of the ion velocity distribution function can be obtained by linearizing Eq. (3) to give

$$\frac{f_1(u,x,t)}{\Delta n}=\begin{cases} f_0(u)-C_s^2f_0'(u)\int_{-\infty}^{x/t}\frac{h_0(\gamma)}{u-\gamma}d\gamma\,, & \text{for } x/t<u\,,\\ C_s^2f_0'(u)\int_{x/t}^{\infty}\frac{h_0(\gamma)}{u-\gamma}d\gamma\,, & \text{for } x/t>u\,,\end{cases} \tag{4}$$

with $C_s^2\equiv T_e/M$ and $n_1(x,t)\equiv\int_{-\infty}^{\infty}f_1(u,x,t)du$. The distribution function $f_1(u,x,t)$ has an integrable singularity for $x/t=u$. There are no singularities for the integrations in Eq. (4). We introduced $h_0(\zeta)\equiv-d(n_1(\zeta)/\Delta n)/d\zeta$ for simplicity. After some algebra[5,18] (see also Sec. IV A), we find for linearly stable plasmas

$$h_0(\gamma)\equiv\frac{1}{\pi}\Im\left\{\left(P\int_{-\infty}^{\infty}\frac{f_0(u)}{u-\gamma}du+i\pi f_0(\gamma)\right)\times\left(1-C_s^2P\int_{-\infty}^{\infty}\frac{f_0'(u)}{u-\gamma}du-i\pi C_s^2f_0'(\gamma)\right)^{-1}\right\}, \tag{5}$$

where $\Im\{\}$ denotes the imaginary part of the expression in the brackets $\{\}$, and $P\int$ denotes the principal value of the integral. We illustrate $h_0(\gamma)$ in Fig. 1 for the reference case of $f_0(u)$ being a Maxwellian. Here, we can introduce the plasma dispersion function[19] and obtain $h_0(\gamma)$ analytically. In particular, for $T_e = 0$ we find $h_0(\gamma) = f_0(\gamma)$, giving the free streaming results as for a Knudsen gas. In the present quasi-neutral limit, charge separations are completely shielded by cold electrons, and the entire plasma dynamics is then controlled by the ion pressure.

The analytically obtained velocity distribution function $f_1(u,x,t)$ has to be added to the background distribution $f_0(u)$, so it is not unphysical to have $f_1(u,x,t) < 0$. The singularity at $u = x/t$ is an artifact resulting from the linearization together with the idealized initial condition consisting of a Heaviside step-function.

The space-time evolution of the perturbation in ion density is obtained as

$$n_1(x,t) = \Delta n \int_{x/t}^{\infty} h_0(\gamma) d\gamma, \tag{6}$$

while the corresponding perturbation of the ion flux $F_1(x,t)$ is obtained from the ion continuity equation in the general self-similar form

$$-\zeta \frac{\partial n}{\partial \zeta} + \frac{\partial F}{\partial \zeta} = 0. \tag{7}$$

Inserting Eq. (6), we find

$$F_1(x,t) = \Delta n \int_{x/t}^{\infty} \gamma h_0(\gamma) d\gamma. \tag{8}$$

The density as well as the ion flux evolves self-similarly in the present limit for any velocity distribution $f_0(u)$, just as the perturbation of the ion velocity distribution function.[3,5,8,9]

We presented linear analytical results for the density, ion flux, and average ion velocity. More generally, the linearized version of Eq. (2) gives

$$(u-\zeta)\frac{\partial}{\partial \zeta} f_1 - C_s^2 \frac{\partial n_1}{\partial \zeta} f_0'(u) = 0. \tag{9}$$

Inserting Eq. (6), we can also obtain more complicated expressions, such as

$$\int_{-\infty}^{\infty} u^2 f_1(u,x,t) du = \Delta n \left(\int_{-\infty}^{\infty} u^2 f_0(u) du + \int_{-\infty}^{x/t} (C_s^2 - \gamma^2) h_0(\gamma) d\gamma \right), \tag{10}$$

found by multiplying Eq. (9) with u and integrating. A term containing $\int_{-\infty}^{\infty} u f_1 du$ is rewritten by use of Eq. (8). An integration constant is given by $\int_{-\infty}^{\infty} u^2 f_1(u,x,t) du \to \Delta n \int_{-\infty}^{\infty} u^2 f_0(u) du$ for $x/t \to -\infty$. Recall that $f_1(u,x,t)$ represents a deviation from $f_0(u)$ and can take negative values also.

The analytical form (6) is shown in Fig. 2(a) for two temperature ratios $T_e/T_i = 3$ and $T_e/T_i = 6$, for a reference Maxwellian ion distribution with no drift velocity. In the density evolution, we can distinguish the forward propagating signal and the backward moving rarefaction wave. At the origin, we have at all times $n_1 = \frac{1}{2}\Delta n$ for symmetry reasons. Note that the rarefaction wave prevails also in the limit of

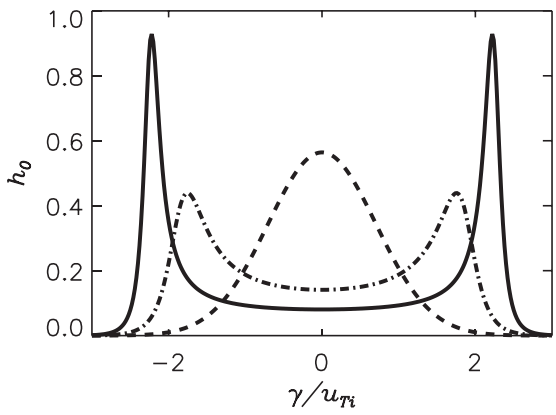

FIG. 1. Illustration of the function $h_0(\gamma/u_{Ti})$ as given by Eq. (5), here shown for the reference case where $f_0(u)$ is a Maxwellian with no drift velocity. The normalizing velocity is defined as $u_{Ti} = \sqrt{2T_i/M}$. Results are shown for two temperature ratios, $T_e/T_i = 6$ (full line) and $T_e/T_i = 3$ (dotted-dashed line). For reference, we show also the result for $T_e = 0$ with a dashed line. The area covered by the three curves is the same.

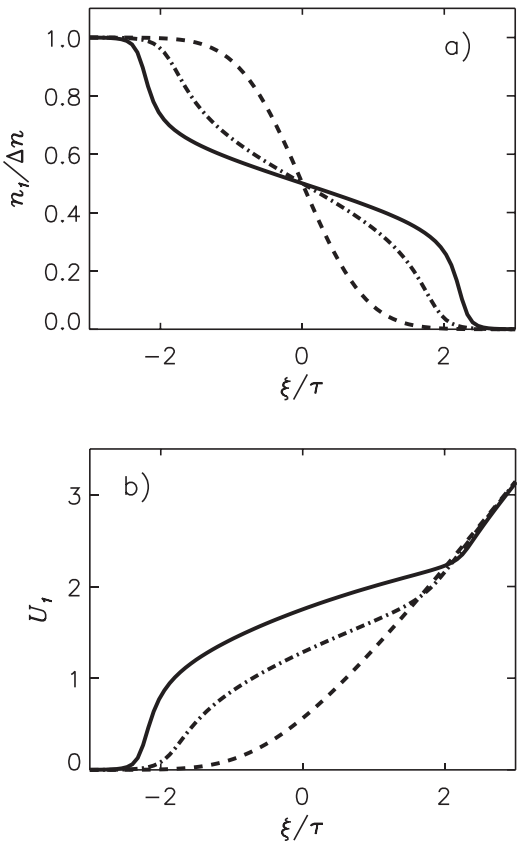

FIG. 2. Illustration in (a): The analytical expression for the evolution of the self-similar normalized density $n_1/\Delta n$ for two temperature ratios, $T_e/T_i = 6$ (full line) and $T_e/T_i = 3$ (dotted-dashed line). The corresponding normalized average ion velocities U_1 are shown in (b). The results are obtained by integrations involving the h_0-function shown in Fig. 1. The ion velocity distribution is here taken to be a Maxwellian with no average drift velocity. For reference, we show also the free streaming Knudsen gas results with dashed lines.

freely streaming ions, i.e., for $T_e = 0$ for instance with a Maxwellian $f_0(u)$. As the electron-ion temperature ratio increases, we note a steepening of the density variation. For the free streaming solution, we find a constant sign for the curvature for $x/t > 0$ and $x/t < 0$, respectively. For the two temperature ratios shown, we note a change in curvature in the two ranges mentioned. The separating case is $T_e/T_i = 1$. For $T_e/T_i \to \infty$, the forward and backward propagating signals will approach the step-functions found by the corresponding fluid analysis. Due to the assumption of Boltzmann distributed electrons, the density perturbation is directly proportional to the electrostatic potential in the present small amplitude, quasi-neutral limit. The electric field is given as $E = -\partial\phi/\partial x = -(T_e/en_0)\partial n/\partial x$. According to Eq. (6), we then have $E(x/t) \sim h_0(x/t)$ as shown in Fig. 1.

The space-time varying local average ion velocity is given as the ratio of the ion flux and the ion density, which by use of Eqs. (6) and (8) gives

$$U_1(x,t) \equiv \frac{F_1(x,t)}{n_1(x,t)} = \frac{\int_{x/t}^{\infty} \gamma h_0(\gamma) d\gamma}{\int_{x/t}^{\infty} h_0(\gamma) d\gamma}, \tag{11}$$

independent of Δn. For illustration of U_1, see Fig. 2(b). For $x/t \to \infty$, we find that this velocity increases without limit, although the density of these fast particles becomes small since $n_1(x,t) = \Delta n \int_{x/t}^{\infty} h_0(\gamma) d\gamma \to 0$ here. We find it interesting to note that the asymptotic limit of $U_1(\zeta \to \infty)$ is the same for all T_e/T_i, even in the absence of collective interaction (i.e., $T_e = 0$). The few particles experiencing the large initial electric fields are accelerated to high velocities, i.e., velocities exceeding the ion thermal velocity u_{th}. The present result is thus consistent with other studies,[1] where it is argued that a small number of ions get accelerated to very high velocities in front of an expanding plasma pulse. The results in Fig. 2 include also the free streaming result: we note that the fastest particles (i.e., the largest U_1 found at large ξ) in the present model are freely streaming, corresponding to a ballistic motion. One limitation of the analysis is found in the assumption of Boltzmann distributed electrons: for large local ion velocities this assumption brakes down, but as said, this limitation affects only a small number of ions. For very large average ion velocities, the present simplified self-similar model breaks down, but we find the trend shown in Fig. 2(b) interesting.

The phase space variation of the ion velocity distribution is illustrated in Figs. 3 and 4 for the two temperature ratios $T_e/T_i = 3$ and $T_e/T_i = 6$ analyzed before. The analysis assumes as in Fig. 2 that the unperturbed ion velocity distribution $f_0(u)$ is a Maxwellian. If we integrate the distributions in Figs. 3 and 4 with respect to velocity u, we obtain the density variations shown in Fig. 2. The figures illustrate how particles are accelerated by the collective electric fields, giving a surplus for positive velocities and a corresponding deficit for negative velocity regions. The collective electric fields are stronger for larger temperature ratios: if we take $T_e/T_i = 1$, we see very little difference as compared to the case with $T_e = 0$, indicating that dispersion by free streaming ions dominates the space-time plasma evolution for $T_e/T_i \leq 1$.

We show results for the illustrative reference case where $f_0(u)$ is a Maxwellian with vanishing average velocity. Results for a drifting Maxwellian are easily obtained by a change in the origin of the x/t-axis and the velocity axis in Figs. 3 and 4.

Concerning normalization of these and following results we note that with a Maxwellian velocity distribution an ion thermal velocity enters as a natural unit for velocity normalization. In the present self-similar limit, there are no natural length or time scales, so we can normalize position and time with the ion Debye length λ_i and the ion plasma period $1/\omega_{pi}$, respectively, but we can choose the combination $\alpha\lambda_i$ and α/ω_{pi} as well, with arbitrary values of α. In the following, we choose $\alpha = 1$ also when normalizing collision frequencies. We thus have normalized relative positions $\xi \equiv (x - x_g)/\lambda_i$ and $\tau \equiv (t - t_0)/\omega_{pi}$ in terms of a reference position x_g and a reference time t_0, so that the ratio ξ/τ is normalized by C_s.

III. NUMERICAL SIMULATIONS

The numerical studies are carried out by a PIC simulation using a code described elsewhere.[20] We formulate the

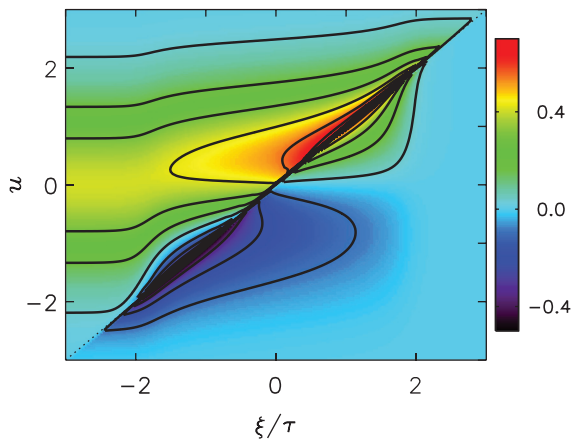

FIG. 3. Color coded ion velocity distribution for $T_e/T_i = 3$, obtained for the reference case with $f_0(u)$ being a Maxwellian ion velocity distribution, see also Figs. 1 and 2.

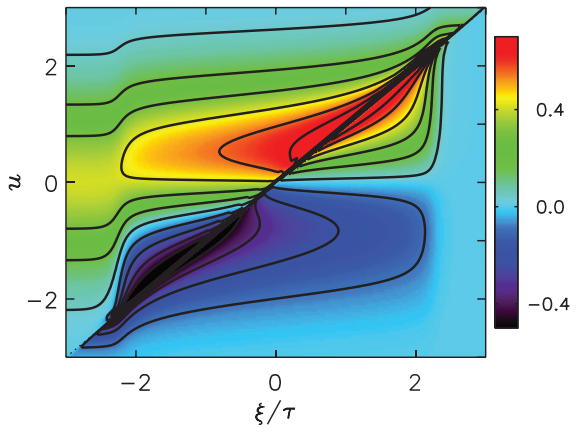

FIG. 4. Color coded ion velocity distribution for $T_e/T_i = 6$. See also Fig. 3.

problem and its boundary conditions so that it applies for the operation of a single ended Q-machine,[14,21] where electrons are emitted thermally, while ions are produced by surface ionization at a hot cathode. Under steady state conditions, the ion velocity distribution in the main plasma (outside the end-sheaths) is a truncated Maxwellian.[14] In the basic version of the Q-machine, the ions are produced by contact ionization[22] of hot alkali metals with suitable work functions.[23] The metal plate also supplies electrons by Richardson emission. We will in the following assume that a confining homogeneous axial magnetic field is sufficiently strong to justify a description in one spatial dimension.

Assuming standard operating conditions for a Q-machine in our simulations, we use electron rich conditions, where the hot plate at $x=0$ can supply electrons in abundance. The electrons are emitted with a velocity distribution $n_{0e}\sqrt{m/2\pi T_0}\exp(-\frac{1}{2}mu^2/T_0)$ for $u>0$, where T_0 is the hot plate temperature in energy units, and similarly for the ions we have $n_{0i}\sqrt{M/2\pi T_0}\exp(-\frac{1}{2}Mu^2/T_0)$ for $u\geq 0$. Our reference case corresponds to $n_{0e}/n_{0i}=1/3$. For such cases, the plasma assumes a negative potential in front of the cathode in order to reflect the surplus of electrons, while ions on the other hand are accelerated by the potential drop to give a net ion flow through the device. A step-like initial condition is obtained by absorbing a part of the ions passing through a grid at a reference position at $x=x_g$. At a time when a steady state condition is achieved, we have a step-like condition with an ion density $n_0+\Delta n$ for $x<x_g$ and n_0 for $x>x_g$, where Δn depends on the absorption rate. At a reference time t_0, the ion absorption is cancelled and the initial density discontinuity is allowed to evolve freely. This condition can be realized in a Q-machine by immersing a fine meshed grid at $x=x_g$. The ion absorption can be controlled by an externally applied potential.[5,18] The physical conditions summarized here are those being simulated by use of our PIC code.[20]

In Video 1, with corresponding still-figure or "snapshot" in Fig. 5, we show an illustrative case with 50% ion absorption at the reference positions $x_g=0$. We initialize the analysis by an empty plasma column. First, we see the filling-up of the plasma, and when a steady state condition has been obtained, we stop the ion absorption at $t=t_0$ and the entire ion-population is allowed to expand into the region $x>0$. The code is general, and does not make use of quasi-neutral assumptions, so we observe the Debye shielding with the electron density extending a distance of the order of λ_{De} into the region $x>x_g$ at times $t<t_0$. The electron-rich sheaths at the two ends of the plasma column are noticeable.

The self-similar nature of the space-time evolution is shown best by a video. In this case, we use the video as a diagnostic tool and not merely for illustration. After the reference time t_0 where the ion absorption is stopped, we continuously rescale the x-axis to show the figure as a function $(x-x_g)/(t-t_0)$, see Video 2. See also still-figure or snapshot in Fig. 6. The code allows also the electron time-scale to be resolved. We note that after a short transient time interval of the order of $1/\omega_{pe}$, the space-time evolution becomes nearly self-similar: this is evidenced by the velocity distribution as well as the potential becoming stationary when represented as functions of $(\xi/\tau)/C_s=(x-x_g)/(t-t_0)$. For small $\Delta n/n_0$, we find that the self-similar variation is nearly perfect for $t>1/\omega_{pe}$. For the nonlinear case in Video 2 (see also Fig. 6), we note at late times a "detachment" of the distribution function from the line $u=x/t$ for velocities $u\leq u_{th}$, the ion thermal velocity, resulting in a "void" in phase space. For large velocities, where the phase space

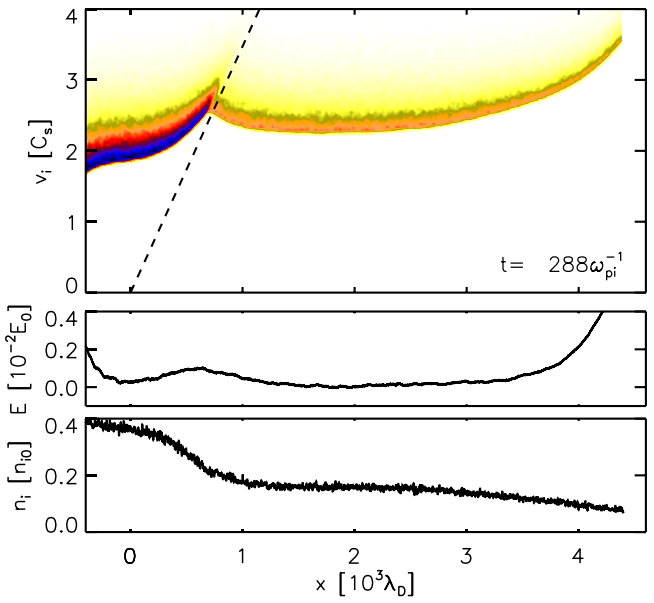

FIG. 5. We show here the space-time evolution of ion phase-space, the electric field, and the ion density for a case where $\Delta n/n_0=0.50$. The dashed line gives $u=x/t$ for reference. The code does not assume quasi-neutrality and Poisson's equation is retained for generality. We can consequently observe the Debye shielding of the charge surrounding the absorbing grid up to a distance of the order of λ_{De} (enhanced online) [URL: http://dx.doi.org/10.1063/1.4816953.1].

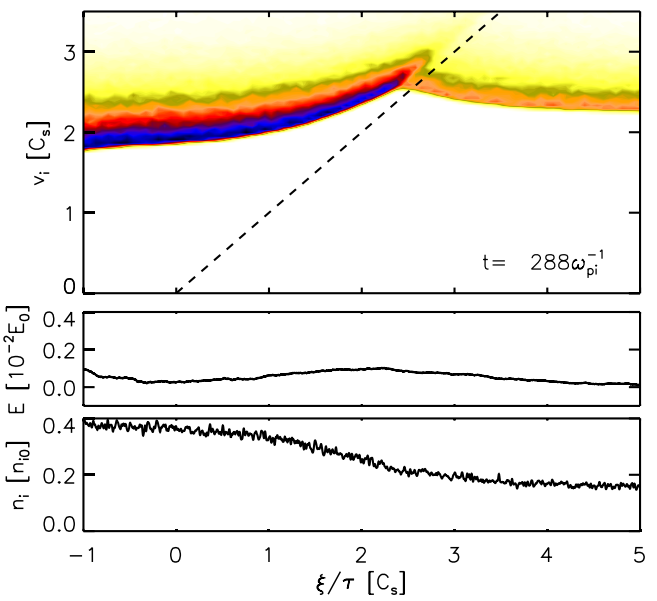

FIG. 6. We show here a restricted part of the space-time evolution in Video 1 (see Fig. 5), now in terms of the normalized self-similar variable ξ/τ. We have $\Delta n/n_0=0.5$. Only a part of the axis is shown, since the two electron rich sheaths at the ends of the plasma column are not accounted for in the present analysis (enhanced online) [URL: http://dx.doi.org/10.1063/1.4816953.2].

density is small, we find that the self-similarity remains to a good approximation. This nonlinear effect was anticipated by analytical studies.[9]

In Fig. 7, we show "snap-shots" or still-figures of ion phase-space, electric field, and ion density all obtained at $t - t_0 = 112\omega_{pi}^{-1}$. Note that for the conditions relevant, for instance, for Q-machines, there is no symmetry in the distribution of particles faster and slower than the average velocity, respectively. The symmetry found in, for instance, Fig. 2 for the forward and backward propagating density variations will be lost. The self-similarity of the solution is, however, independent of any symmetry conditions (see Sec. II) and will remain. We can give a simple illustration of the loss of symmetry by considering the freely streaming ions, which is included in Eq. (4) for $T_e = 0$. Taking $f_0(u) = (1/a)\exp(-\frac{1}{2}Mu^2/T_i)$ for $u > u_{min}$ and $f_0(u) = 0$ for $u < u_{min}$ for some minimum velocity u_{min} (as in our simulations and in most Q-machine experiments[14]), we have the normalization constant $a = \sqrt{\pi/2}\sqrt{T_i/M}\big(1 - \text{erf}\,(u_{min}\sqrt{M/2T_i})\big)$, and $n(x,t) = \Delta n\sqrt{\pi/2}\sqrt{T_i/M}\big(1 - \text{erf}\,(\sqrt{M/2T_i}\,x/t)\big)/a$ for $x/t \geq u_{min}$ and $n(x,t) = \Delta n$ for $x/t < u_{min}$.

A. Nonlinear effects

The analysis in Sec. II applies for small perturbations only. By the numerical simulations, we can study the deviations from these results as the amplitude Δn of the perturbation is increased. For illustration, we show in Fig. 7 results from four simulations with different values of Δn. For the smallest perturbation level $\Delta n = 0.1$, we improve the signal-to-noise ratio by taking the average of four runs with different initializations of the random number generators injecting the particles. The singular line $u = x/t$ remains in the velocity distribution also for nonlinear perturbations as anticipated by expression (3) derived from first principles with the given approximations. For moderate temperature ratios, $T_e/T_i \leq 6$, the results for $\Delta n/n_0 \leq 0.25$ are in good agreement with what we expect from a linearized analysis, as also found in related laboratory experiments.[5]

In Fig. 8, we illustrate the space-time evolution of a condition with a relatively large initial perturbation, here $\Delta n/n_0 = 0.5$. The figure illustrates the most conspicuous nonlinear effect found in the density evolution, namely ions reflected by the propagating density step. The velocity of these reflected particles is close to twice the step velocity,

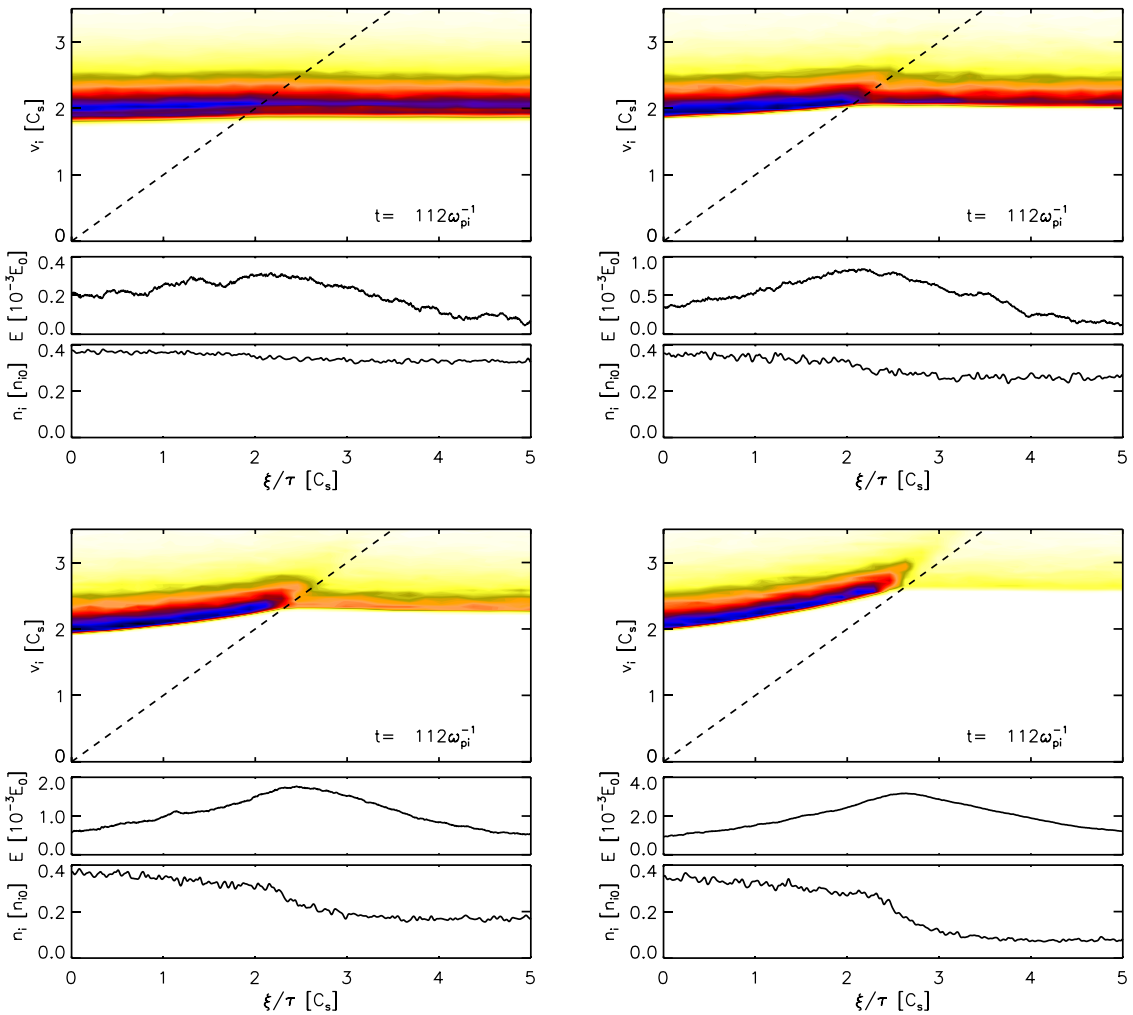

FIG. 7. Illustrations of results for the ion velocity distributions, variations of electric fields, and density for varying perturbation amplitudes, as functions of $\xi/\tau \equiv x/t/C_s$, here with $\Delta n/n_0 = 0.10$, 0.25 (top left and right) 0.5, and 0.75 (bottom left and right). A dashed line in the phase-space representation gives $u = x/t$, with the origin being at the reference grid position. The figures are all obtained at a time $112\,\omega_{pi}^{-1}$.

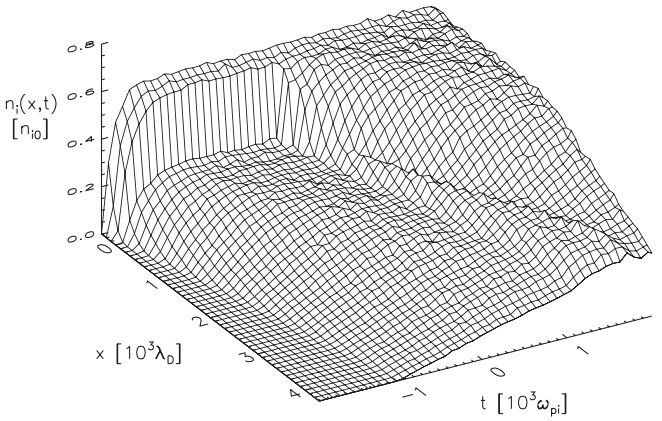

FIG. 8. Space-time evolution of the ion density in the numerical simulations of a collisionless plasma. The figure shows the initial filling-in of the system, with a step discontinuity with $\Delta n/n_0 = 0.5$, which is released at $t = 0$. Note the small amplitude precursor that propagates with approximately twice the speed of sound. The figure is obtained by average of 30 realizations with different initializations of the random number generators.

i.e., approximately $2C_s$. In order to improve the signal-to-noise ratio in Fig. 8, we averaged 30 runs with identical macroscopic conditions but different initializations of the random number generators. Otherwise, the reflected particles would be masked by the fluctuation due to discrete particle effects.

IV. THE EFFECTS OF NEUTRAL COLLISIONS

To account for collisional interactions, the ion Vlasov equation is often modified by a simple collision term as $-\nu\big(f(u,x,t) - n_0 f_0(u)\big)$, or its generalizations. In the present study, we distinguish elastic ion collisions with neutrals, and charge exchange collisions. Both cases are studied numerically. For the latter processes, we can obtain a closed analytical solution by introducing a physically realistic collision model in the ion Vlasov equation.

Analytical results using a general energy conserving Bhatnagar–Gross–Krook (BGK)-model in a kinetic description can be found in the literature,[24,25] but these results refer to discontinuities initiated by a moving piston. Here, we outline analytical results directly applicable for the present initial value problem. For some special cases, the results become remarkably simple.

A. Analytical models for charge-exchange collisions

Consider a model for charge exchange collisions based on a simple collisional term of the form $-\nu(f_1 - n_1 f_0(u))$, where again $n_1 \equiv \int f_1 du$ and $\int f_0(u)du = 1$. In linearized form, the collision term becomes $-\nu(f_1 - f_0(u)n_1)$ to be added to the right hand side of the linearized ion Vlasov equation. It turns out to be relatively easy to retain a velocity dependence of the collision frequency $\nu = \nu(u)$ within the following analysis. The integral transforms found in the following can, however, no longer be expressed in terms of known functions, and the practical value of the results will be limited. We, therefore, here take ν to be constant, and make the transformation $f_* \equiv f_1 \exp(\nu t)$, giving $n_* \equiv n_1 \exp(\nu t)$, to find

$$\frac{\partial}{\partial t} f_* + u\frac{\partial}{\partial x} f_* - \frac{T_e}{M}\frac{\partial n_*}{\partial x}\frac{\partial}{\partial u} f_0(u) - \nu f_0(u) n_* = 0. \tag{12}$$

A constant value for ν implies that the collisional cross sections vary as $\sigma \sim 1/u$ with varying velocity, and serves only as a solvable convenient model for charge exchange collisions. More generally, we have, however, that polarization forces ("Maxwellian molecules") give constant ν for a wide range of velocities[26] so the model as such is not unphysical.

After a temporal Laplace transform (with complex s) and spatial Fourier transform (with real k) of Eq. (12), we have

$$(s + iku) f_*(k,u,s) - n_*(k,s)\left(ik\frac{T_e}{M} f_0'(u) + \nu f_0(u)\right) = f_*(k,u,t=0) = i\frac{\Delta n}{k} g(u), \tag{13}$$

or

$$f_*(k,u,s) = i\frac{\Delta n}{k}\frac{g(u)}{s+iku} + n_*(k,s)\frac{ikC_s^2 f_0'(u) + \nu f_0(u)}{s+iku}, \tag{14}$$

giving

$$n_*(k,s) = \frac{i\frac{\Delta n}{k}\int \frac{g(u)}{s+iku}du}{1 - \int \frac{ikC_s^2 f_0'(u) + \nu f_0(u)}{s+iku}du}, \tag{15}$$

where $g(u)$ is the velocity distribution in the perturbation for $x < 0$. Integration limits are omitted for simplicity: they are $\int_{-\infty}^{\infty} du$ in all cases shown. The ensuing method of solution can be used for this general case, but a remarkable simplification results by taking $g(u) = f_0(u)$. In this case, the analysis contains only one nontrivial complex function, which can then be related to the plasma dispersion function for a Maxwellian choice of $f_0(u)$. The solution of the problem is then obtained by methods outlined in the literature.[27] We have

$$n_*(k,s) = \frac{\Delta n}{k^2}\frac{h_*(is/k)}{1 + i(\nu/k)h_*(is/k)} \equiv \frac{\Delta n}{k^2} N_*(k,s), \tag{16}$$

where we introduced the complex function

$$h_*(is/k) \equiv \frac{\int \frac{f_0(u)}{u - is/k}du}{1 - C_s^2\int \frac{f_0'(u)}{u - is/k}du}.$$

For the ensuing inverse transforms, we note that for $k < 0$ the singularity at $is/k = u$ is *below* the u-axis for the velocity integration, while it is *above* for $k > 0$. To distinguish the two cases, we introduce the notation $n_*^{(1)}(k,s)$ for $k < 0$ and $n_*^{(2)}(k,s)$ for $k > 0$.

We have

$$n_*(x,s) = \frac{1}{2\pi}\int_{-\infty}^{0} \frac{\Delta n}{k^2} N_*^{(1)}(k,s) e^{ikx} dk + \frac{1}{2\pi}\int_{0}^{\infty} \frac{\Delta n}{k^2} N_*^{(2)}(k,s) e^{ikx} dk$$

and

$$n_*(x,t) = \frac{1}{i2\pi}\int_{s_0-i\infty}^{s_0+i\infty} n_*(x,s)e^{st}ds,$$

where $s_0 > 0$. The inverse Fourier transform is separated into two parts, $-\infty < k \le 0$ and $0 \le k < \infty$ as shown. We introduce the variable $\gamma \equiv is/k$ with γ real, giving $d\gamma = -is\,dk/k^2$. With this choice, we have h_* to be a function of a real variable, i.e., $h_* = h_*(\gamma)$, and we also have $N_*(k,s) \to N_*(\gamma,s) = h_*(\gamma)/(1+(\nu/s)\gamma h_*(\gamma))$. Deforming the integration contour as shown in Fig. 9, we find

$$n_*(x,s) = \frac{\Delta n}{2\pi}\int_0^\infty \frac{N_*^{(1)}(\gamma,s) - N_*^{(2)}(\gamma,s)}{is} e^{-sx/\gamma}d\gamma. \qquad (17)$$

The integrals along the circular contours in Fig. 9 vanish when $R \to \infty$. The integrations along the two closed contours shown (containing I and III, and II and IV, respectively) are vanishing. We note that we have a zero for the denominator of $n_*(\gamma,s)$ for $s = -\nu\gamma h_*(\gamma)$, recalling that, in general, $h_*(\gamma)$ is a complex function of real γ.

For linearly stable plasmas, the inverse Laplace transform of

$$\frac{h_*(\gamma)}{1+(\nu/s)\gamma h_*(\gamma)}\frac{e^{-sx/\gamma}}{is}$$

is determined to give the final result in the form

$$\begin{aligned} n_*(x,t) &= \frac{\Delta n}{2\pi} i\int_{x/t}^\infty [h_*^{(2)}(\gamma)\exp\big(t\nu(\gamma - x/t)h_*^{(2)}(\gamma)\big) \\ &\quad - h_*^{(1)}(\gamma)\exp\big(t\nu(\gamma - x/t)h_*^{(1)}(\gamma)\big)]\,d\gamma \\ &= \frac{\Delta n}{\pi}\int_{x/t}^\infty [\Im\{h_*^{(2)}(\gamma)\}\cos(\Im\{h_*^{(2)}(\gamma)\}t\nu(\gamma - x/t)) \\ &\quad - \Re\{h_*^{(2)}(\gamma)\}\sin(\Im\{h_*^{(2)}(\gamma)\}t\nu(\gamma - x/t))] \\ &\quad \times \exp\big(-\Re\{h_*^{(2)}(\gamma)\}t\nu(\gamma - x/t)\big)\,d\gamma, \end{aligned} \qquad (18)$$

where the two functions $h_*^{(2)}(\gamma)$ and $h_*^{(1)}(\gamma)$ are complex conjugates and $\Im\{h_*^{(2)}(\gamma)\}/\pi \equiv h_0(\gamma)$. By $\Re\{\}$, we understand the real part of the function in the brackets. Expression (18) is strongly simplified in the limit $\nu \to 0$, and we recover here the special case (6) where we use definition (5). The self-similar x/t-dependence is lost when $\nu \neq 0$, see Fig. 10. For short times, $t \ll 1/\nu$ we have solutions close to the previous

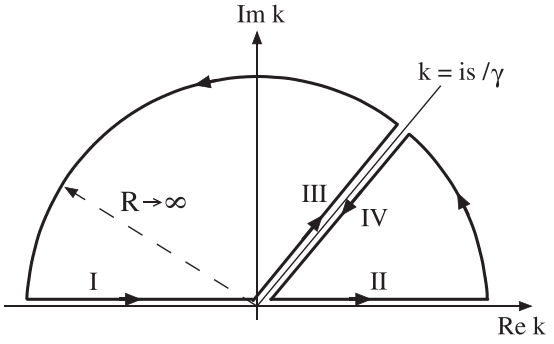

FIG. 9. Integration contours in the complex k-plane.

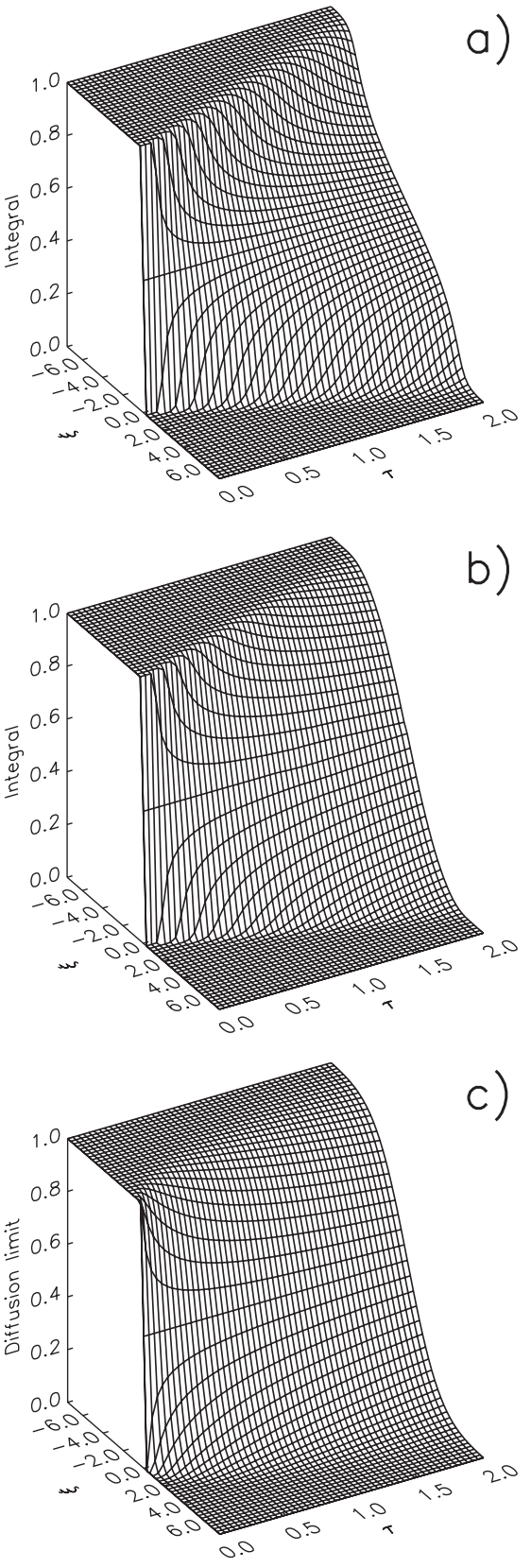

FIG. 10. The space-time evolution of the normalized plasma density $n/\Delta n$ for a step-like initial perturbation with $T_e/T_i = 3$, including collisional effects with $\nu/\omega_{pi} = 2$ is shown in (b). For reference, we show the collisionless case with $\nu = 0$ in (a) and the corresponding solution for the diffusion equation in (c), where the normalized diffusion coefficient is here $D \equiv (C_s/u_{ti})^2/(\nu/\omega_{pi})$. For large times, we find that the density variations shown in (b) and (c) are almost identical, while for short times the density variations in (a) and (b) are almost identical.

self-similar result, but for later times deviations develop, and the solution approaches the form characterizing diffusion equations.

The result (18) may at first sight appear complicated. In reality, it contains only elementary functions in addition to $h_0(\gamma)$ which, in turn, can here be expressed by the Z-function[19] for Maxwellian velocity distributions or sums of such. The integral in Eq. (18) is readily carried out numerically, the only complication being the oscillatory integrand.

For the velocity distribution function we find by Eq. (12), where now $n_*(x,t)$ is known

$$f_*(x,u,t)/\Delta n = g(u)\mathcal{H}(u-x/t) + C_s^2\frac{\partial f_0(u)}{\partial u}\int_0^t \frac{\partial n_*(x-u(t-t'),t')}{\partial x}dt' + \nu f_0(u)\int_0^t n_*(x-u(t-t'),t')\,dt', \tag{19}$$

where the first term (containing Heaviside's step function $\mathcal{H}$) corresponds to the free streaming contribution from the initial perturbation, here taken as $g(u) = f_0(u)$. The final results are obtained as $n_1 = n_* e^{-\nu t}$ and $f_1 = f_* e^{-\nu t}$. Since the self-similarity of the solution is lost for large times when $\nu \neq 0$, we no longer have any singularity at $x/t = u$: it is smoothed over by the collisions. The time-integrations in Eq. (19) are not easily carried out analytically due to the $\int_{x/t}^{\infty} d\gamma$-integral entering the expression for the density. For large times, the most significant contribution to $f_*(x,u,t)$ comes from the last term in Eq. (19).

Results based on Eq. (19) are shown as ion phase-space diagrams in Fig. 11 for 2 different times for a normalized spatial variable. For $t < 1/\nu$, the results are almost indistinguishable from that shown in Fig. 3 in agreement also with experimental results[5] where the space-time evolution of ion velocity distributions was measured. For late times, on the other hand, we find a collision-dominated evolution of the velocity distribution function. The case with high collision frequency is illustrated in Fig. 12, to be compared to Fig. 11. The two figures are obtained at the same time in units of ω_{pi}^{-1}, but the collision frequency is doubled in Fig. 12.

Result (19) together with (18) offers a theoretical result which, albeit somewhat complicated, allows for illustrating a continuous transition from a collisionless to a collision-dominated space-time evolution of the ion velocity distribution for the given step-like initial condition.

B. Strongly collisional regime

Using $n_1 = n_* e^{-\nu t}$ and $f_1 = f_* e^{-\nu t}$ and integrating Eq. (12) with respect to u, we obtain the continuity equation for n_1. Multiplying the expressions with u and integrating as before, we have the momentum equation. Assuming $T_e \gg T_i$ and large ν, this expression contains Fick's first law in the form $nU \approx -(C_s^2/\nu)\partial n/\partial x$, where U is the average ion velocity for the perturbation. Using this expression in the continuity equation, we obtain a diffusion equation for the plasma density with diffusion coefficient $D \equiv C_s^2/\nu$. When the collisional mean free path is the shortest length scale in the system (i.e., shorter than the length-scale for the density gradient), we can approximate the dynamics by a simple diffusion equation having the relevant solution in the form

$$n_1(x,t) = \frac{\Delta n}{2}\left(1 - \mathrm{erf}\left(\frac{x}{\sqrt{4Dt}}\right)\right), \tag{20}$$

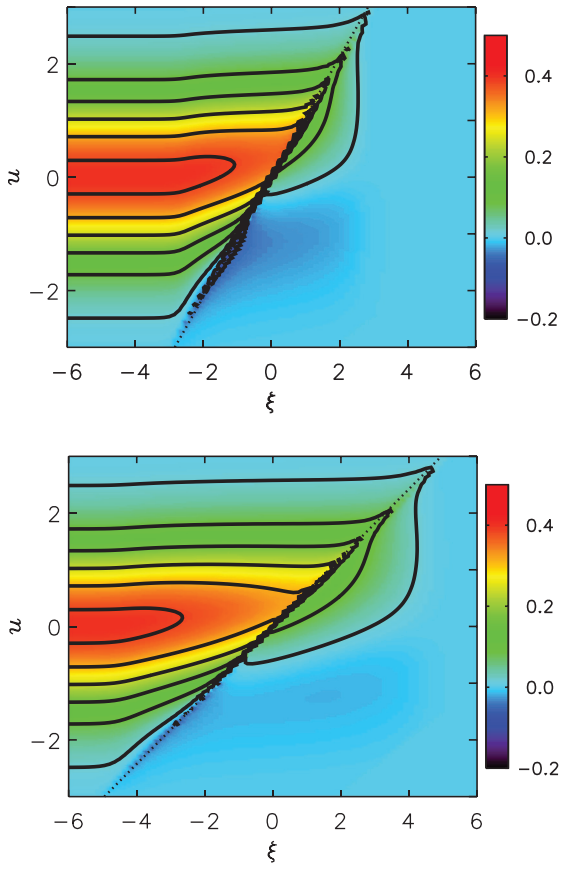

FIG. 11. Analytical results for the ion velocity distribution in normalized phase-space, as obtained from Eq. (19) with $\nu \neq 0$ and $T_e/T_i = 3$. We show the phase-space for two times, $t = 0.5/\nu$ and $0.85/\nu$. The dotted line shows $u = x/t$, for reference. Note that the evolution is no longer self-similar. The figures are to be compared to the collisionless case shown in Fig. 3 obtained with the same temperature ratio.

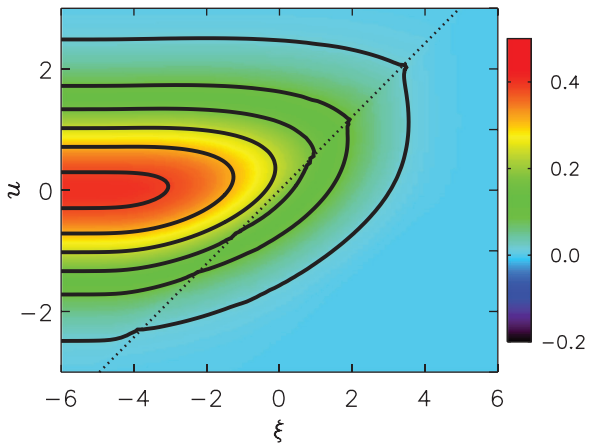

FIG. 12. Analytical results for the ion velocity distribution in normalized phase-space with doubled collision frequency as compared to Fig. 11. Other parameters are the same as in Fig. 11.

in terms of the error function, $\mathrm{erf}(x) \equiv (2/\sqrt{\pi})\int_0^x e^{-y^2} dy$. In this limit, we have a dynamic length scale $\sqrt{Dt}$ characterising the time evolution of the initial condition, and the self-similar variable x/t from the analysis in Sec. II is lost. In the diffusion limit, the ion velocity distribution remains close to $f_0(u)$, which for realistic conditions is a Maxwellian with constant temperature T_i. Result (20) is shown for reference in Fig. 10(c).

We note that Eq. (19) with $f_1 = f_* e^{-\nu t}$ offers a general relation between the plasma density and the ion velocity distribution function as described by the ion Vlasov equation with collisional effects included. We analyzed also the ion velocity distribution for late times obtained by using the analytical form (20) in Eq. (19). The result obtained for $f_1(x,u,t)$ by this procedure is almost identical to the late time expression obtained analytically with collisional effects retained in Eq. (12). We confirmed also here that for large times the most significant contribution to $f_1(x,u,t)$ comes from the last term in Eq. (19).

V. NUMERICAL RESULTS FOR PLASMAS WITH CHARGE EXCHANGE COLLISIONS

We analyze the effects of ion neutral collisions numerically, and consider two cases: elastic and charge exchange collisions between the plasma ions and a neutral background. Also other types of collisions can be important, but we expect these two to be representative for collisional interactions in general.

Charge exchange collisions often have the largest cross section, this type of interaction being resonant,[28] and will be particularly important for many realistic cases.

In Fig. 13, we show the space-time evolution of the plasma density for two cases, where $\ell_c = 1000$ and $500\,\lambda_{De}$, respectively. The absorbing grid is placed at $x = 0$. The filling in of the plasma column (including the effect of the charge exchange collisions) begins at $t = -2$ as in Fig. 8, and the step-like density perturbation is released at $t = 0$. We find that the signal has an enhanced noise level due to the collisions, although 30 realizations are averaged as in Fig. 8. Note that the step-like front found in Fig. 8 is no longer present, as expected from the analytical results. Rather we find (for both mean free paths shown) a monotonically decreasing plasma density as in Fig. 10(c). Due to the charge exchange collisions, the average ion flow velocity is reduced along the axis. Flux conservation of the ion flow from the origin (the hot plate in a Q-machine) along the x-axis will give rise to an enhancement of the plasma density as compared to the case without collisions.

In Fig. 14, we show numerical results (to be compared with the phase-space results for the collisionless simulations in Fig. 7 and density variations in Fig. 8) with charge exchange effects included. We show results for two collisional mean free paths, in both cases with $\Delta n/n_0 = 1/2$. The most conspicuous effect of the collisions is that the step-like front seen in, for instance, Fig. 10 disappears, and is replaced by a variation closer to the one given by Eq. (20). The neutral component is taken to be at rest, and we see the formation of a slow ion component composed by particles that has

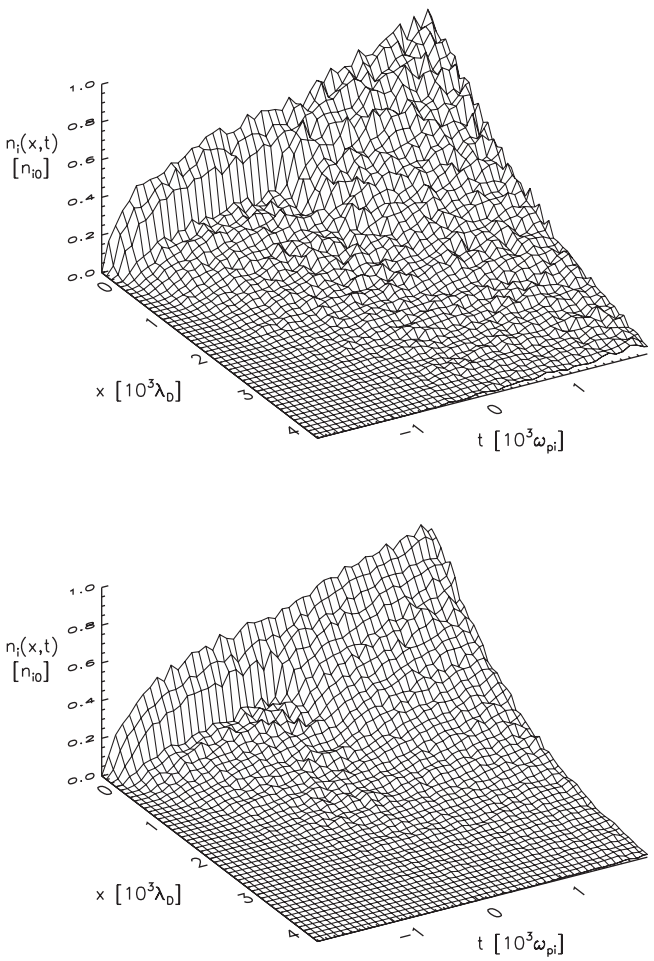

FIG. 13. Space-time variation of the plasma density with charge exchange collisions included, with mean free path $\ell_c = 1000$ (top) and $500\,\lambda_{De}$ (bottom). Both cases have $\Delta n/n_0 = 0.5$. As compared to Fig. 8, the signal has an enhanced noise level due to the collisions, although 30 realizations are averaged also here as in Fig. 8. The absorbing grid is placed at $x = 0$. The filling in of the plasma column (including the effect of the charge exchange collisions) begins at $t = -2$ as in Fig. 8, while the step-function is released at $t = 0$.

undergone a charge exchange collision. This is seen best for the smallest mean free path, $\ell_c = 500\,\lambda_{De}$. The average velocity of these particles is positive, since they are also accelerated by the collective electric fields. In Video 3 (see also corresponding "snap-shot" in Fig. 15), we show the space-time evolutions for density, electric field, and ion phase-space. Note how the self-similarity disappears as time increases.

One basic conclusion from the collisional simulations is that a laboratory experiment for realizing a step-like initial condition is best performed for a collisionless case: we find that the charge exchange collisions induce an inhomogeneous plasma density along the axis of the device and the ideal unperturbed state is not obtained. We find, however, a qualitative agreement with the analytical results.

Our code also allows for inclusion of elastic ion collisions. Also, these processes have been studied numerically, and some differences can be noted, but need not be presented here, since our analytical model applies best for the charge exchange collisions.

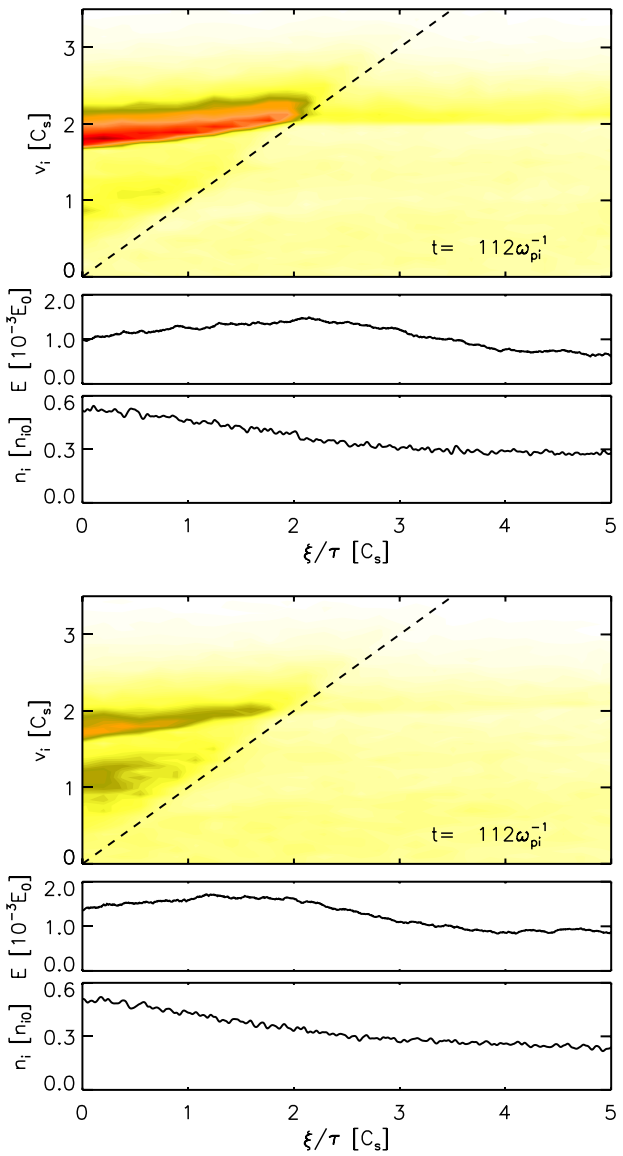

FIG. 14. Numerical simulations with charge exchange collisions, with mean-free collision paths $\ell_c = 1000$ and $500\,\lambda_{De}$.

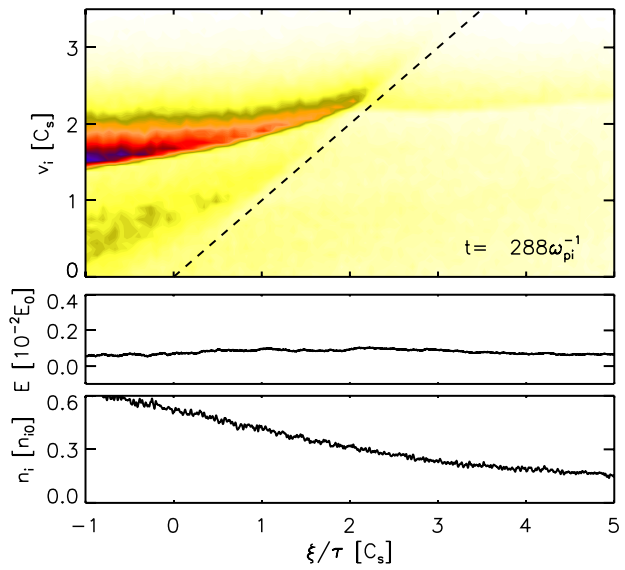

FIG. 15. Numerical simulations where charge exchange collisions are included. We show the space-time evolution of the ion density (bottom frame) electric field (middle frame) and the phase-space for the ion velocity distribution (top frame) for a case where $\Delta n/n_0 = 0.50$, with mean-free collision paths $\ell_c = 1000$ (enhanced online) [URL: http://dx.doi.org/10.1063/1.4816953.3].

VI. DISCUSSIONS

The results in the present work are formally obtained without assumptions on the ratio T_i/T_e. In principle, they apply to Q-machine conditions as well as those met in, for instance, Double Plasma (DP) devices. With the assumption of quasi-neutrality, we do not have the Debye length in the basic equations and we do not recover the dispersive ripples associated with the time evolution of an initial discontinuity.[29] For Q-machine experiments, we have typically an effective temperature ratio in the range $1 < T_e/T_i \leq 3$, so the dispersive ripples are heavily ion Landau damped in those cases. The restriction by the assumed quasi-neutrality is of minor importance in these cases and we find that the results in the present paper are in excellent agreement with the experimental results obtained in a Q-machine[5] also concerning experimentally obtained ion velocity distributions. For larger temperature ratios, it might be an advantage to retain Poisson's equation. Also, this analysis has been carried out in one spatial dimension.[27,30] In this case, the self-similarity of the solution is lost: self-similarity is a property of problems without any characteristic length and time scales. In the quasi-neutral limit of kinetic ion-acoustic waves, we have neither the ion plasma frequency nor the Debye lengths as characteristic quantities; all we have is a characteristic velocity, C_s.

Our numerical results confirmed the analytically obtained self-similar space-time evolution. The theoretical results were illustrated for the special reference case where the unperturbed ion velocity distribution is a full Maxwellian. This case is facilitated by allowing the plasma dispersion function[19] to be introduced. The actual unperturbed ion velocity distribution is a truncated Maxwellian. The symmetry of the forward propagating density pulse and the backward propagating rarefaction wave found in the reference case is lost in our simulations, but the forward propagating density enhancement, and the potential and electric field derived from it, follow the analytical results well.

The time evolution of an initially step-like perturbation in plasmas with large electron-to-ion temperature ratios was investigated by a very elegant method in a DP-device.[31] In this case, the initial perturbation was introduced by a collimated "flash" of light from a vacuum spark between Molybdenum electrodes. The intense light ionizes a fraction of the neutral background gas in the device, and thus produces a "slab" of additional plasma to the pre-existing uniform background plasma produced by the standard DP-operation. Because of the large temperature ratio, the dispersive ripples were clearly observable in this experiment. By a quasi-neutral approximation, such ripples are in effect smoothed out in the analytical results presented in our analysis.

We extended our analysis by introducing ion collisions. Analytical results were obtained by a linearized model with charge exchange collisions. We can follow the transition from the short time collisionless limit to the long time

collisional case, with some basic results shown in Fig. 10. We find it interesting that with a Maxwellian plasma the collisional term contributes with an expression given via the plasma dispersion function, even in the case where collective interactions are turned off by setting $T_e = 0$. Formally, it is a simple matter to retain a velocity dependence of the collision frequency by having a $\nu = \nu(u)$ factor entering the integrands, but then the Hilbert transforms can no longer be easily expressed in terms of the plasma dispersion function, and the practical value of the results is limited. The analytical result (18) contains the collisionless self-similar linearized kinetic result by setting $\nu = 0$, while it for large times, $\nu t \gg 1$, contains the results for a diffusion equation that also has an exact solution (20). These three results are summarized in Fig. 10.

The linearized analysis was carried out for a step-like initial condition. By differentiating this result with respect to the spatial variable x, we can obtain the results for the space-time evolution of an initial $\delta(x)$-perturbation. From this result, arbitrary spatially distributed initial perturbations can be constructed. In this sense, our linear analytical results have general applicability for collisionless as well as collisional plasmas for cases where charge exchange is dominant.

When comparing our results to numerical or laboratory experimental observations, we note that the presentation based on figures such as Figs. 2–4 or Fig. 10 is easy when shown as a function of position for fixed times. For most laboratory studies, it is easier to visualize a temporal variation for fixed position,[5] and in such cases the figures can be redrawn with advantage.

The present analytical results are exact for a linearized model equation, derived from the Vlasov equation including a collision term. The results are thus *not* obtained by use of some first or least damped pole approximation for the entire plasma dispersion relation. Since we used a linearized analysis, the results are not directly applicable, for instance, for plasma expanding into vacuum,[1] but we believe the results to have value as qualitative indications also for this case. This latter problem has received attention for experimental conditions with imposed initial conditions[6] but it can also be relevant for plasma flowing into the wake forming behind macroscopic solid objects immersed in plasmas at large relative flow velocities.[11,12,32,33]

ACKNOWLEDGMENTS

This work was supported in part by a grant from the Norwegian National Science Foundation. We thank Dr. Wojciech Miloch for his interest and for many valuable discussions on numerical problems.

[1]J. E. Crow, P. L. Auer, and J. E. Allen, "Expansion of a plasma into a vacuum," J. Plasma Phys. **14**, 65–76 (1975).
[2]Yu. V. Medvedev, "Ion front in an expanding collisionless plasma," Plasma Phys. Controlled Fusion **53**, 125007 (2011).
[3]Y. Huang, Y. Bi, X. Duan, X. Lan, N. Wang, X. Tang, and Y. He, "Self-similar neutral-plasma isothermal expansion into a vacuum," Appl. Phys. Lett. **92**, 031501 (2008).
[4]R. W. Gould, "Excitation of ion–acoustic waves," Phys. Rev. **136**, A991–A997 (1964).
[5]P. Michelsen and H. L. Pécseli, "Propagation of density perturbations in a collisionless Q-machine plasma," Phys. Fluids **16**, 221–225 (1973).
[6]V. Vanek and T. C. Marshall, "Ion-acoustic collisionless shocks in a Q-machine," Plasma Phys. **14**, 925–934 (1972).
[7]H. K. Andersen, N. D'Angelo, P. Michelsen, and P. Nielsen, "Investigation of Landau-damping effects on shock formation," Phys. Rev. Lett. **19**, 149–151 (1967).
[8]A. L. Gurevich, L. I. Pariĭskaya, and L. P. Pitaevskiĭ, "Self similar motion of rarefied plasma," J. Exp. Theor. Fiz. (U.S.S.R.) **49**, 647–654 (1965) [see also Sov. Phys. JETP 22, 449–454 (1966)].
[9]A. L. Gurevich, L. I. Pariĭskaya, and L. P. Pitaevskiĭ, "Self similar motion of a low-density plasma. II," Zh. Eksp. Teor. Fiz. **54**, 891–904 (1968) [see also Sov. Phys. JETP 27, 476–482 (1968)].
[10]J. Denavit, "Collisionless plasma expansion into a vacuum," Phys. Fluids **22**, 1384 (1979).
[11]T. Nakagawa, "Ion entry into the wake behind a nonmagnetized obstacle in the solar wind: Two-dimensional particle-in-cell simulations," J. Geophys. Res., [Space Phys.] **118**, 1849–1860, doi: 10.1002/jgra.50129 (2013).
[12]N. Singh and R. W. Schunk, "Numerical calculations relevant to the initial expansion of the polar wind," J. Geophys. Res. **87**, 9154–9170, doi:10.1029/JA087iA11p09154 (1982).
[13]D. Grésillon and P. L. Galison, "Instantaneous electron energy distribution function in ion waves," Phys. Fluids **16**, 2180–2183 (1973).
[14]R. W. Motley, *Q Machines* (Academic Press, New York, 1975).
[15]S. Børve, H. L. Pécseli, J. Trulsen, and S. Longo, "Kinetic instabilities associated with injection of a plasma beam into a neutral background," Phys. Scr. **T122**, 125–128 (2006).
[16]B. D. Fried and A. Y. Wong, "Stability limits for longitudinal waves in ion beam-plasma interaction," Phys. Fluids **9**, 1084–1089 (1966).
[17]H. L. Pécseli, *Waves and Oscillations in Plasmas* (Taylor & Francis, London, 2012).
[18]S. A. Andersen, G. B. Christoffersen, V. O. Jensen, P. Michelsen, and P. Nielsen, "Measurements of wave-particle interaction in a single ended Q-machine," Phys. Fluids **14**, 990–998 (1971).
[19]B. D. Fried and S. D. Conte, *The Plasma Dispersion Function* (Academic Press, New York, 1961).
[20]V. L. Rekaa, H. L. Pécseli, and J. K. Trulsen, "Numerical studies of a plasma diode with external forcing," Phys. Plasmas **19**, 082115 (2012).
[21]T. Klinger, F. Greiner, A. Rohde, and A. Piel, "Nonlinear dynamical behavior of thermionic low-pressure discharges. 2. Experimental," Phys. Plasmas **2**, 1822–1836 (1995).
[22]I. Langmuir and K. H. Kingdon, "Thermionic effects caused by vapors of alkali metals," Proc. R. Phys. Soc., Ser. A **107**, 61–79 (1925).
[23]H. B. Michaelson, "The work function of the elements and its periodicity," J. Appl. Phys. **48**, 4729–4733 (1977).
[24]R. J. Mason, "Weak shock generation according to the energy-conserving Bhatnagar-Gross-Krook kinetic equation," Phys. Fluids **13**, 1467–1472 (1970).
[25]R. J. Mason, "Electric field penetration into a plasma with a fractionally accommodating boundary," J. Math. Phys. **9**, 868–874 (1968).
[26]B. A. Trubnikov, "Particle interactions in fully ionized plasmas," in *Reviews of Plasma Physics*, edited by M. A. Leontovich (Consultants Bureau, New York, 1965), Vol. 1, pp. 105–204.
[27]R. J. Mason, "Structure of evolving ion-acoustic fronts in collisionless plasmas," Phys. Fluids **13**, 1042–1048 (1970).
[28]S. A. Andersen, V. O. Jensen, and P. Michelsen, "Charge-exchange cross-sections measured at low energies in Q machines," Rev. Sci. Instrum. **43**, 945–947 (1972).
[29]G. B. Whitham, *Linear and Nonlinear Waves* (John Wiley & Sons, New York, 1974).
[30]R. J. Mason, "Computer simulation of ion-acoustic shocks. The diaphragm problem," Phys. Fluids **14**, 1943–1958 (1971).
[31]D. B. Cohn and K. R. MacKenzie, "Electrostatic ion-acoustic shocks produced by density steps," Phys. Rev. Lett. **28**, 656–658 (1972).
[32]W. J. Miloch, H. L. Pécseli, and J. Trulsen, "Numerical studies of ion focusing behind macroscopic obstacles in a supersonic plasma flow," Phys. Rev. E **77**, 056408 (2008).
[33]S. Kimura and T. Nakagawa, "Electromagnetic full particle simulation of the electric field structure around the moon and the lunar wake," Earth, Planets Space **60**, 591–599 (2008).